Performance Analysis and Data Processing for the Mars Sample Recovery Helicopter in the Jet Propulsion Laboratory 25-ft Space Simulator

Natasha Schatzman
Aerospace Engineer
NASA Ames Research Center
Moffett Field, CA, USA

Athena Chan
Mechanical Engineer
Science and Technology Corporation
Moffett Field, CA, USA

Michael Fillman
Aeromechanical Engineer
AeroVironment, Inc
Simi Valley, CA, USA

Larry Meyn
Aerospace Engineer
NASA Ames Research Center
Moffett Field, CA, USA

Vinod Gehlot
Robotics Systems Engineer
NASA Jet Propulsion Laboratory
Pasadena, CA, USA

Kenneth Glazebrook
Mechatronics Engineer
NASA Jet Propulsion Laboratory
Pasadena, CA, USA

Diego Santillan
Electrical Engineer
NASA Jet Propulsion Laboratory
Pasadena, CA, USA

Paulina Ridland
Aeromechanical Engineer
AeroVironment, Inc
Simi Valley, CA,USA

ABSTRACT

On April 19, 2021, Ingenuity became the first helicopter to fly on Mars at Jezero Crater, completing a total of 72 flights by the end of its mission. The success of Ingenuity resulted in various research efforts to further explore Mars via vertical flight, including two optimized Ingenuity-sized helicopters proposed to retrieve samples for the 2028 Mars Sample Return mission. To aid in the design process for the two proposed Sample Retrieval Helicopters, both heritage and optimized, increased diameter rotors were tested at the NASA Jet Propulsion Laboratory in the 25-ft Space Simulator. Three test campaigns were performed using the Ingenuity rotors and optimized Sample Retrieval Helicopter (SRH) rotors for several rotor speeds, densities, configurations, and collectives to identify performance limitations. These three test campaigns included the Ingenuity Engineering Design Model 1 (EDM-1) with and without a cruciform box, Transonic Rotor Test (TRT) rig, and SRH Dual Rotor Test (DRT). Experimental setup, test matrix, data processing, data quality, and performance results for EDM-1, TRT, and DRT campaigns are presented and discussed. Experimental results from the test campaigns will aid in future experimental methods and validation efforts for planetary rotorcraft exploration.

NOTATION

A	Rotor area (m^2)
C_P	Rotor power coefficient, $\frac{P}{\rho A(\Omega R)^3}$
C_Q	Rotor torque coefficient, $\frac{Q}{\rho A(\Omega R)^2 R}$
C_T	Rotor thrust coefficient, $\frac{T}{\rho A(\Omega R)^2}$
$\frac{C_T}{\sigma}$	Blade loading
$c_{.75}$	Chord at 0.75R (m)
DRT	Dual Rotor Test
$EDM-1$	Engineering Design Model 1
FM	Figure of merit, $\frac{C_T^{3/2}}{\sqrt{2}C_P}$
FTS	Force-torque sensor
f_b	Filter frequency (Hz)
JPL	Jet Propulsion Laboratory
$LAIR$	Lift-off Adapter and Inverted Retention
MSR	Mars Sample Return
M_{tip}	Rotor hover tip Mach number
N_b	Number of blades
P	Shaft power (W)
$P_{electric}$	Electrical power (W)
Q	Shaft torque (N-m)
R	Rotor radius (m)
Re	Reynolds number at 0.75R, $\frac{\rho 0.75 V_{tip} c_{.75}}{\mu}$
RPM	Rotor rotational speed (rev/min)
SRH	Sample Retrieval Helicopter
T	Thrust (N)
TRT	Transonic Rotor Test
t	Time (s)
V_{tip}	Tip speed (m/s)
μ	Dynamic viscosity of the fluid $(\mathrm{kg/m\text{-}s})$
ρ	Air density $(\mathrm{kg/m}^3)$
σ	Rotor solidity, $\frac{N_b c_{.75}}{\pi R}$
$\overline{\sigma}$	Standard deviation
Ω	Angular velocity (rad/s)

Presented at the Vertical Flight Society's 80th Annual Forum & Technology Display, Montréal, Québec, Canada, May 7–9, 2024.

INTRODUCTION

Ingenuity first flew at Mars Jezero Crater on April 19th, 2021, becoming the first helicopter to fly on another planet; it has completed 72 flights (Ref. 1). A photo captured by Mars rover Perseverance on August 2nd, 2023 is shown in Fig. 1.

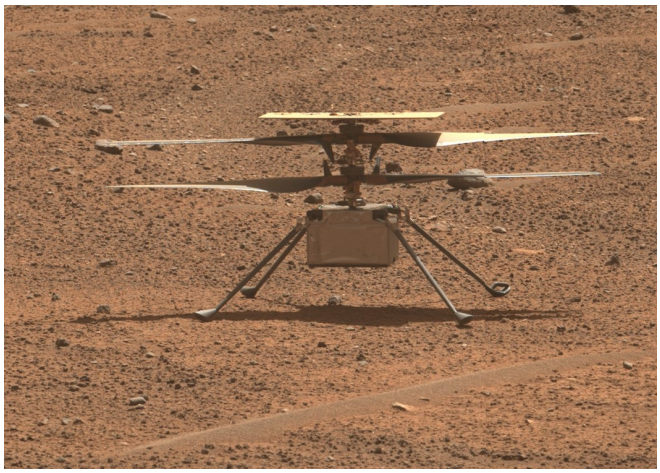

Figure 1. Ingenuity at Mars Jezero Crater. (Credit: NASA / JPL-Caltech / ASU / MSSS.)

The success of Ingenuity resulted in the possible use of two helicopters to retrieve samples for the proposed NASA and ESA (European Space Agency) Mars Sample Return (MSR) mission. The objective of the MSR mission is to collect Mars regolith samples and deliver them back to Earth by the mid 2030's. Use of the proposed helicopters would operate as a back-up in the event that Perseverance is not operational. Currently, Perseverance is collecting samples and storing them for future retrieval either by the rover itself or from a cached depot (Ref. 2).

Due to the increased lift requirement created by carrying the sample payloads, three design parameters were explored in this work that included increasing blade collective pitch, rotational speed, and blade radius of the Ingenuity rotor.

An optimized rotor was developed for the Sample Return Helicopter (SRH) mission. To aid in this development, experimental data was desired to validate the predicted aerodynamic performance across rotor speeds, atmospheric densities, rotor configurations, and blade collectives. Furthermore, the optimized rotor required experimental validation to ensure it met its design requirements of lifting 2.5 kg.

From 2022 to 2023, three rotor test campaigns were conducted at the JPL 25-ft Space Simulator in support of SRH development. The primary objectives of these tests were to determine the performance limits of the heritage Ingenuity rotor blade, and to collect aerodynamic performance data for the new SRH rotor blade design. The Ingenuity tests included the Engineering Design Model 1 (EDM-1) test and the Transonic Rotor Test (TRT) (Ref. 1). The EDM-1 test was further broken down into two experiments: one with a cruciform box, and one without. The cruciform box was used to simulate the Lift-off Adapter and Inverted Retention (LAIR) box, which is the initial takeoff platform on Mars for the SRHs. The inclusion of the cruciform box enabled data collection for rotor-on-LAIR aerodynamic interactions. The EDM-1 test article was a vehicle near-identical to Ingenuity except for the pitch links, which were modified to reach higher collective angles to identify stall and power limits. The Transonic Rotor Test (TRT) features a single rotor setup with the same blade geometry as EDM-1 but designed to spin at much higher rotational speeds; this test focused on determining if compressibility effects would be significant. Compressibility effects were a concern because as rotors enter the transonic regime in Earth conditions ($M_{tip} > 0.7$), rotors tend to experience large increases in blade drag (resulting in increased torque and decreased efficiency) and early onset of blade stall. Ultimately, the EDM-1 and TRT showed that while more thrust could be generated, SRH mission requirement were not met, which motivated the partial redesign of the SRH blades.

In 2023, a SRH rotor design was tested at the JPL 25-ft Space Simulator in support of the MSR mission. These new SRH blades featured changes in twist, chord, and radius compared to the Ingenuity blades. The primary airfoil was maintained as heritage from Ingenuity, see Fig. 2 and Table 1 for geometry specifications. The Dual Rotor Test (DRT) featured two SRH rotors mounted in a coaxial configuration with an inter-rotor separation of approximately 15% rotor radius.

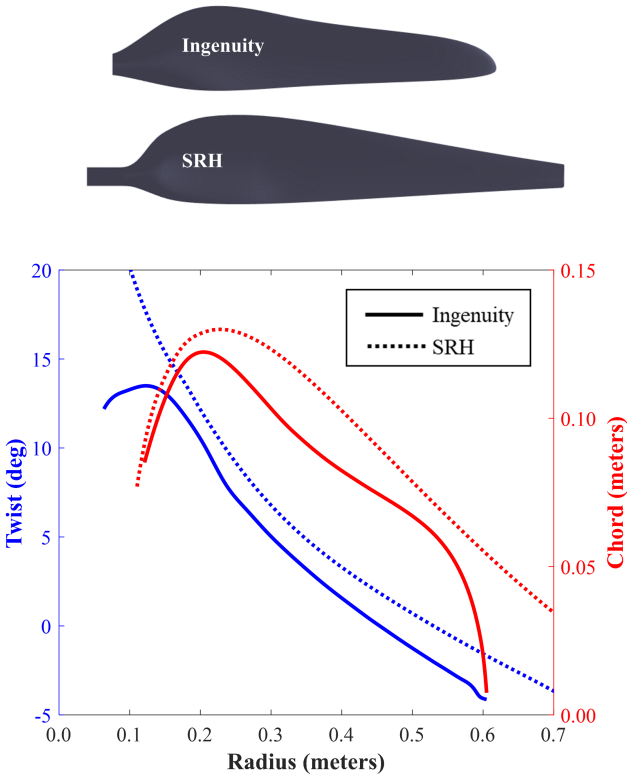

Figure 2. Ingenuity and SRH blade geometry specifications.

Table 1. EDM-1, TRT, and DRT geometry specifications.

Test campaign	EDM-1	TRT	DRT
R (m)	0.605	0.605	0.706
N_b	4	2	4
$c_{.75}$ (m)	0.074	0.074	0.070
σ	0.148	0.074	0.126

TEST SETUP

Test setup in terms of facility, test models, instrumentation, and installation are discussed for the EDM-1, TRT, and DRT campaigns.

Facility

The 25-foot Space Simulator is located at NASA Jet Propulsion Laboratory in Pasadena, California. The test chamber was pumped to vacuum, then backfilled with carbon dioxide and the pressure actively controlled to hit the target Martian density values. The chamber's ambient temperature was monitored and ranged between 19 and 27 degrees Celsius.

Test Models

The EDM-1 test model shown in Fig. 3 without a cruciform box was nearly identical to Ingenuity with the primary difference being the pitch links, which were adjusted to allow for higher collective angles in an effort to identify stall and other limits. EDM-1 included the solar panel, fuselage, and landing gear of Ingenuity.

Figure 3. Engineering Design Model 1 (EDM-1) without cruciform box in the 25-foot Space Simulator.

EDM-1 was also tested with a cruciform box (Fig. 4) to simulate the helicopter taking off from the LAIR box.

The TRT test model consisted of a single rotor setup designed to spin at higher rotational speeds to understand compressibility effects using Ingenuity's rotor geometry (Fig. 5).

The SRH model used an optimized, larger rotor radius rotor with an improved twist and chord distribution, see Fig. 6. Differing from the EDM-1 setup, the DRT and TRT setup did not include a fuselage.

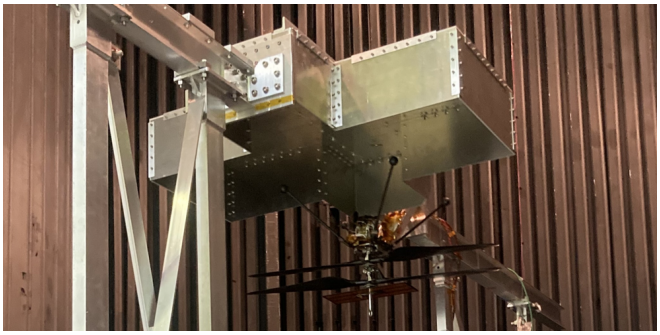

Figure 4. Engineering Design Model 1 (EDM-1) with cruciform box in the 25-foot Space Simulator.

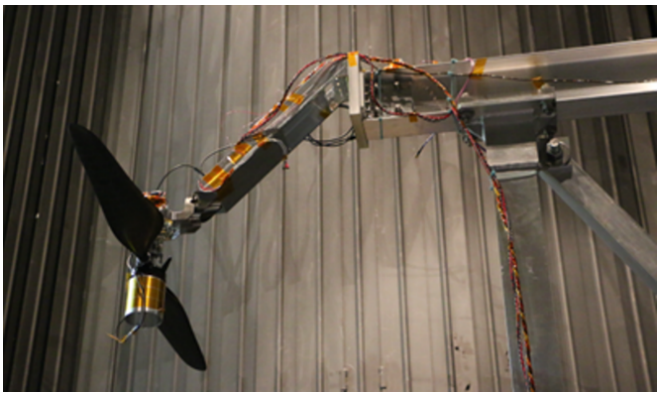

Figure 5. Transonic Rotor Test (TRT) in the 25-foot Space Simulator.

Instrumentation

For safety monitoring, four cameras were placed in the chamber around the model, and one microphone was installed below the rotor on the chamber floor. EDM-1 used two hand-wound, custom Ingenuity-style motors. The TRT rotor system was powered by a single modified Maxon EC 87 motor. Force and torque for both the EDM-1 and TRT tests were measured using a single ATI Mini 45 force-torque sensor (FTS). Note that the single FTS meant forces and torques for each rotor in the EDM-1 test could not be resolved and instead were derived from electrical measurements and calculations.

For DRT, each rotor was powered by its own modified Maxon EC 87 motor. Each motor mounted onto its own respective motor-sensor interface hardware; two ATI Mini 45 force torque sensors were bolted to the other side of each interface. Since the FTSs were not mounted in line with the rotor's reference frame, a transformation matrix was applied to the data sets taken by the FTSs. The matrix application methodology is discussed in the data processing section.

Installation

The rotor system was mounted upside down relative to the chamber's floor to reduce ground effect caused by the downwash. As a result, the rotor that was aerodynamically the

Figure 6. SRH Dual Rotor Test (DRT) in the 25-foot Space Simulator.

upper rotor was physically the bottom rotor in the test set up, and likewise, the aerodynamically lower rotor was physically the top rotor. The upper/lower rotor refers to the rotors as they would be positioned on a flight vehicle; whereas top/bottom rotor refers to where the rotors were placed physically in the test chamber, see Fig. 7. A Mechanical Ground Support Equipment (MGSE) gantry was used to support the test articles. A second MGSE gantry was used to hold the cruciform box over EDM-1 when needed.

TEST MATRIX

A summary of test conditions for all three test campaigns is shown in Fig. 8 and in Table 2. Five distinct types of data runs were conducted: step, sweep, trim, doublet, and triangle collective inputs. Types of runs were defined by how the collective input was applied, see reference (Ref. 1) for further descriptions. Only step runs are presented. Note that experimental densities were selected to most closely match the densities found at potential mission sites and to cover the expected range of Reynolds numbers.

EDM-1 without the cruciform box focused on conducting collective sweeps (1 to 22 degrees) at varying densities (0.0100, 0.0125, 0.0185, and 0.0300 kg/m^3) and RPMs (2043, 2200, and 2550). Chamber temperatures ranged from 18.5 to 22.47 degrees Celsius during testing. Runs included coaxial and single (upper and lower rotor independently) rotor configurations. Since a single FTS was used, independent upper and lower rotor runs were performed to collect "single" rotor electrical power data. An estimated mechanical power curve derived from the measured electrical power was fitted for each rotor for figure of merit calculations.

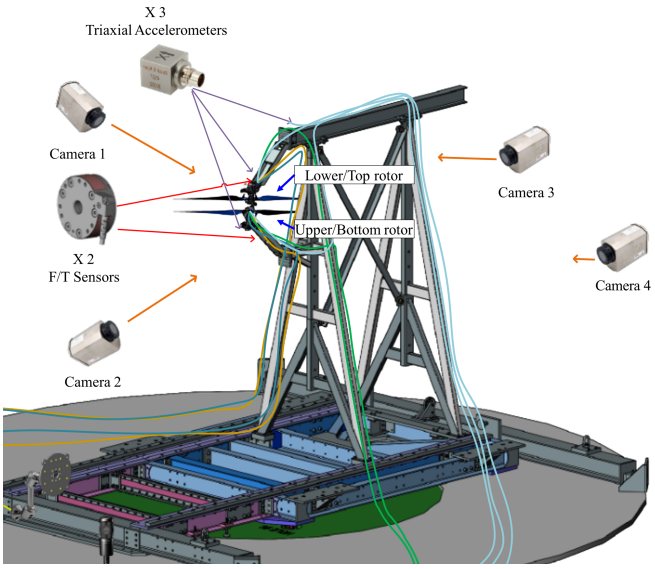

Figure 7. DRT hardware installation and location in 25-ft Space Simulator.

EDM-1 with the cruciform box focused on conducting collective sweeps (1.5 to 21.5 degrees) at varying densities (0.0100, 0.0185, and 0.0300 kg/m^3) and RPMs (2200 and 2043). Chamber temperatures ranged from 17.72 to 22.11 degrees Celsius during testing. Runs only included the coaxial rotor configuration.

TRT focused on conducting collective sweeps (0 to 20 degrees) at a constant density of 0.0100 kg/m^3 and varying RPMs (2740, 2950, 3160, 3375, and 3585). Chamber temperatures ranged from 20.11 to 21.15 degrees Celsius during testing.

The DRT test campaign focused on conducting collective sweeps (-4 to 23 degrees) at different densities (0.0100, 0.0125, and 0.0185 kg/m^3) and varying RPMs (2371, 2544, 2736, 2860, 3101, 3283, 3360, and 3466). Chamber temperatures ranged from 19.16 to 26.4 degrees Celsius during testing. Similar Reynolds numbers were tested for the DRT (green circles in Fig. 8) and TRT (black triangles in Fig. 8) campaigns due to the shared goal of pushing the rotor tip speed to understand performance limitations.

ACQUISITION AND OPERATIONS

Runs were limited to approximately 60 seconds, including startup and shutdown, due to motor thermal limits in the low density environment. Data was acquired continuously during this time. For each run, rotational speed and density were held constant while collective increased/decreased in set increments, holding for 2-3 seconds at each collective.

Five different data acquisition systems were used for each test, which included: helicopter controls (collective and RPM), force and torque sensor, accelerometers, microphone, and thermocouples. Helicopter controls and force-torque data were acquired at 500 Hz.

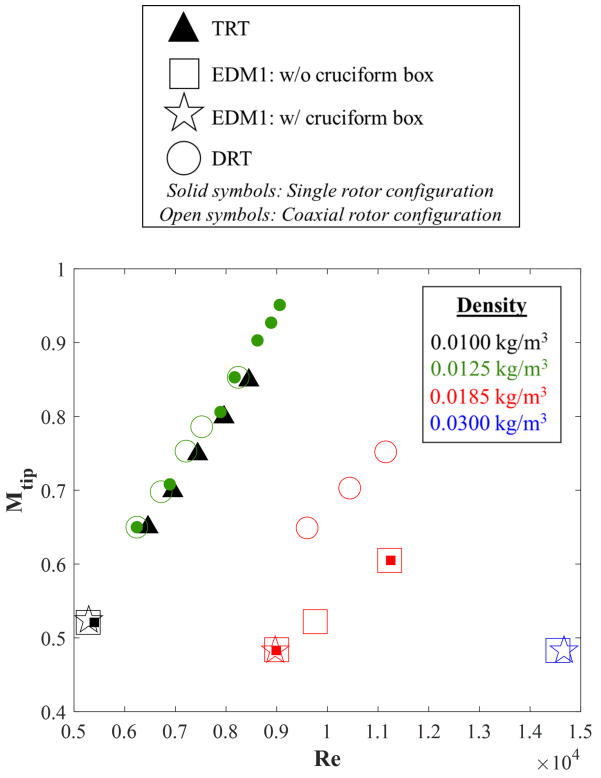

Figure 8. EDM-1, TRT, and DRT test campaign conditions.

The commanded and measured helicopter controls were recorded simultaneously through the same data acquisition system for the upper and lower rotors. However, the FTS measurements were unsynchronized and measured using separate data acquisition systems, thus requiring post-processing to align the acquired data.

For the single rotor test of the DRT, the lower rotor was operated at target values for the run while the upper rotor was operated at a constant 450 RPM and 0 degrees collective. These values were chosen to minimize the effect of the upper rotor on the lower rotor, thereby maintaining a safe and controlled state for the rotor system. Resonance modes of the SRH test stand limited M_{tip} achievable on the upper rotor to 0.85 for this test.

Test operations were as follows for the DRT campaign:

1. Asynchronized data acquisition starts: helicopter control, motor power, force/torque
2. Servo doublet input to aid in data synchronization
3. Collective input of 0 degrees
4. Rotor spun up to nominal startup RPM
5. Collective input of 1.5 degrees
6. RPM set to target speed
7. Collective inputs to aid in data alignment

Table 2. EDM-1, TRT, and DRT test matrix.

Test	Rotor	RPM	Density (kg/m^3)	M_{tip}	Re
	Both	2200	0.0100	0.52	5254
	Upper	2200	0.0103	0.52	5367
	Lower	2200	0.0103	0.52	5404
	Both	2200	0.0141	0.52	7382
EDM-1	Both	2043	0.0184	0.48	8971
w/o	Upper	2043	0.0184	0.48	8895
cruciform	Lower	2043	0.0185	0.48	8986
box	Both	2200	0.0186	0.52	9757
	Both	2550	0.0185	0.60	11230
	Upper	2550	0.0185	0.60	11249
	Lower	2550	0.0185	0.60	11249
	Both	2043	0.0300	0.48	14549
EDM-1 w/	Both	2200	0.0103	0.52	5396
cruciform	Both	2043	0.0185	0.48	8946
box	Both	2043	0.0303	0.48	14674
	Single	2740	0.0099	0.65	6461
	Single	2950	0.0099	0.70	6950
TRT	Single	3160	0.0099	0.75	7437
	Single	3375	0.0099	0.80	7944
	Single	3585	0.0099	0.85	8452
	Both	2371	0.0119	0.65	6240
	Lower	2371	0.0119	0.65	6240
	Both	2544	0.0120	0.698	6720
	Lower	2554	0.0120	0.708	6890
	Both	2736	0.0119	0.753	7210
	Both	2860	0.0119	0.786	7520
DRT	Lower	2918	0.0121	0.806	7890
	Lower	3101	0.0119	0.853	8170
	Both	3101	0.0120	0.853	8240
	Lower	3283	0.0118	0.903	8620
	Lower	3360	0.0118	0.927	8890
	Lower	3466	0.0118	0.951	9060
	Both	2371	0.0184	0.649	9600
	Both	2554	0.0184	0.703	10440
	Both	2736	0.0184	0.752	11150

8. Testing sequence initiated
9. Collective inputs to aid in data alignment
10. RPM ramp down to 0
11. Servo doublet input to aid in data synchronization
12. Rotor and data collection stop

DATA PROCESSING

Data for all test campaigns was processed using MATLAB R2023a (Ref. 4). A summary of data processing steps is shown in Fig. 9.

First, the raw force and torque data were transformed to account for FTS location and orientation. Weight tares were performed by subtracting the mean of the first 2 seconds of FTS data from the subsequent FTS data in each run; the rotors

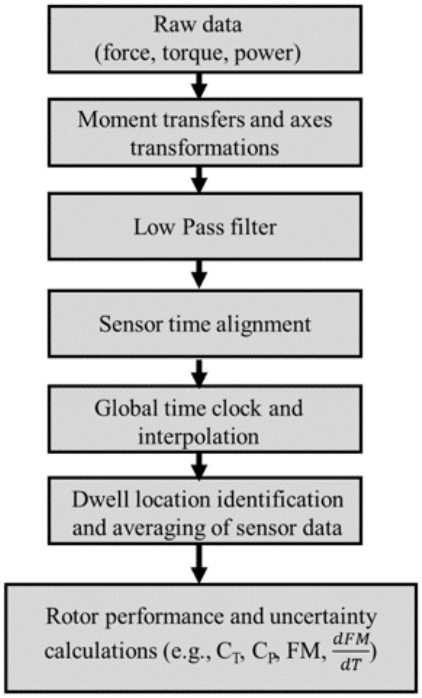

Figure 9. Data processing for DRT campaign.

were not spinning during the first 2 seconds. Due to unwanted high frequency electrical noise and mechanical vibratory content, the raw force and torque data were filtered. A study was performed for a range of low pass frequencies which determined that a 4th order 2 Hz low-pass Butterworth filter was sufficient for removing the unwanted high frequency content, see Fig. 10 a) for entire run and 10 b) for single dwell. A 4th order 2 Hz low-pass Butterworth filter was used to capture abrupt changes in thrust due to collective changes without significantly modifying the measured average thrust.

Since data was not recorded at the same start and end times across all sensors, the data was synchronized by identifying and aligning positive or negative slope changes in collective and thrust. The center of each dwell, or period of constant collective, was identified, and data was averaged for approximately 29 revolutions at this point. Figure 11 a) shows the entire time history of a run and Fig. 11 b) shows a close-up view of a single dwell to highlight the start (green circle) and stop (red circle) of a single dwell, as well as the time window selected for averaging (gray shaded region).

Next, a global time clock with a sampling frequency of 500 Hz was defined based on the maximum start and minimum end time of each parameter time clock, thereby allowing for all data to be interpolated to a consistent 500 Hz time base. The consistent time base ensured all data records had the same length and occurred at the same time. Finally, performance variables such as figure of merit, coefficient of thrust and coefficient of power were calculated along with their uncertainty values.

a)

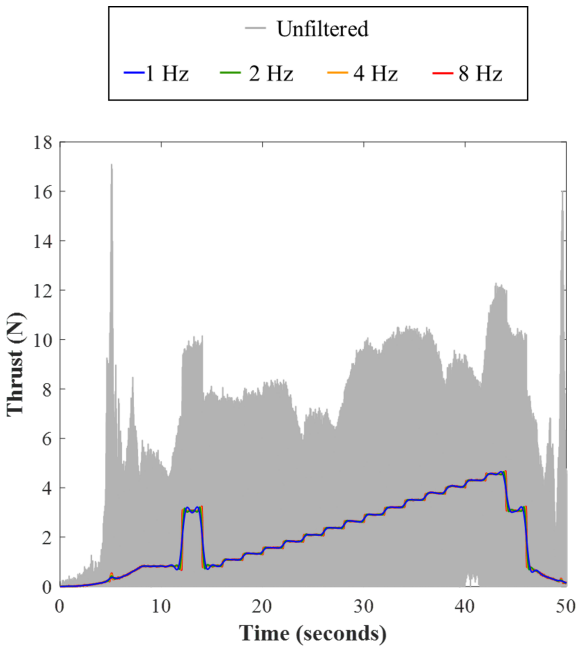

b)

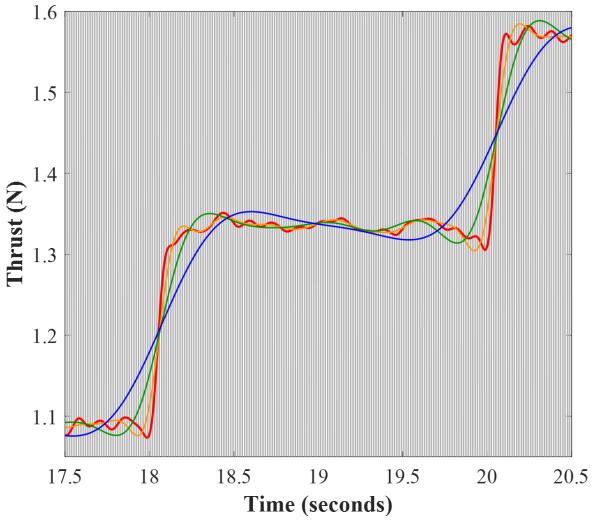

Figure 10. Filter setting identification of a) entire run and of b) single dwell.

RESULTS

Results from the EDM-1, TRT, and DRT campaigns were able to determine if increasing (1) blade collective, (2) RPM, and (3) blade radius, would increase the total lift and meet the proposed SRH mission requirements (Fig. 12). EDM-1 and TRT focused on understanding thrust and RPM limits for the Ingenuity rotor, while DRT explored performance of a larger blade radius. Though the DRT campaign included single rotor runs (Table 2), results will not be presented.

The C_P versus C_T, FM versus C_T/σ, and collective pitch versus C_T/σ figures are presented to help characterize rotor per-

a)

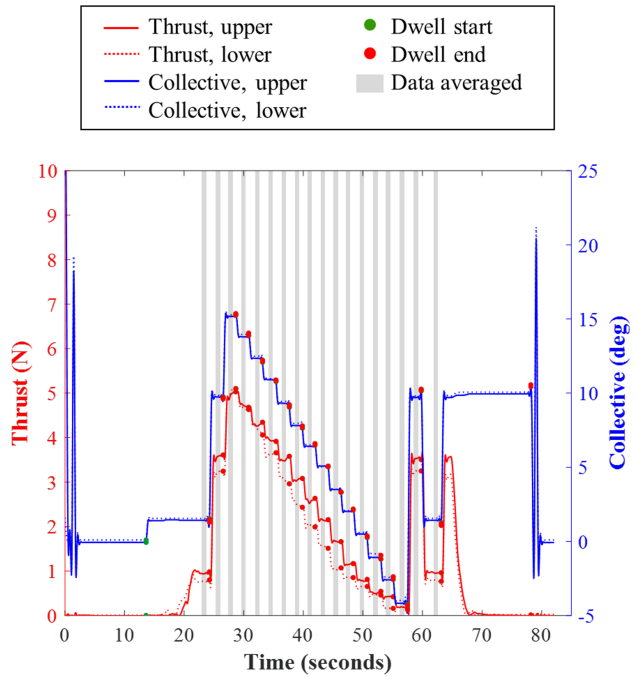

b)

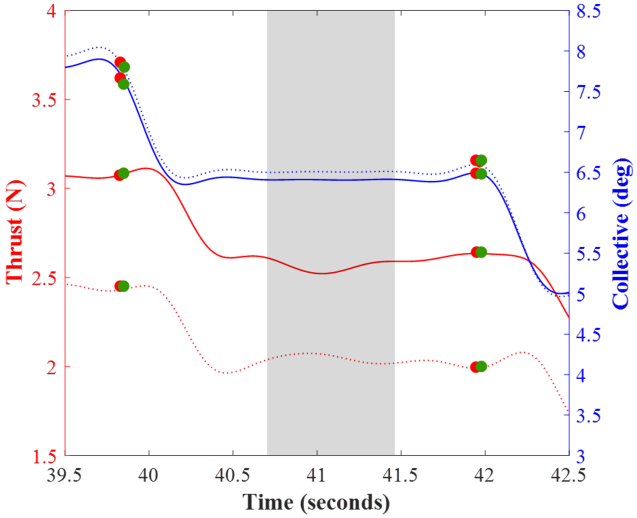

Figure 11. Example time adjusted run data set for upper and lower thrust, collective, and data selected to average for a) entire run and b) zoomed in view.

formance. Figure of merit, which gauges the efficiency of a rotor, is defined as the ratio between the ideal and actual power of the rotor, and is calculated using measured thrust, rotor torque, and density (Ref. 5).

The FM versus C_T/σ data from EDM-1 and TRT of the Ingenuity rotor are plotted in Fig. 12. Results shows a peak figure of merit occurring at a blade loading of 0.13 for the EDM-1 and TRT campaigns. The figure of merit reveals a general trend of improved efficiency as Reynolds number increases. However, the TRT data also suggests compressibility effects begin to slightly reduce the net efficiency once M_{tip} is greater than 0.75. No large reduction in FM was observed to indicate stall of the rotor(s) tested at these flight conditions.

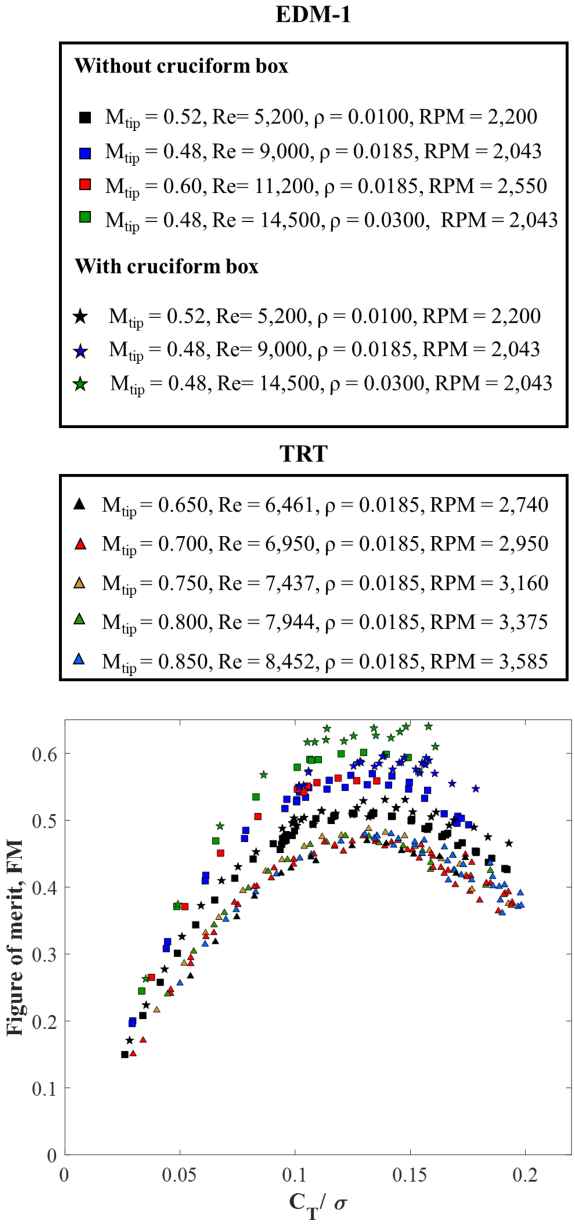

Figure 12. Figure of merit versus blade loading for EDM-1 coaxial configuration with and without cruciform box and TRT.

DRT performance is shown in Fig. 13 for (a) C_P versus C_T and (b) FM versus C_T/σ, respectively. The sensitivity of C_P and FM to M_{tip} appears to be reduced in the DRT compared to the EDM-1 and TRT experiments. However, a larger increase in rotor efficiency can still be seen with the considerable increase in Reynolds number going from a density of 0.0120 kg/m^3 to a density of 0.0185 kg/m^3.

The SRH rotor reached a peak figure of merit between a blade loading of 0.12 and 0.13 for the coaxial configuration. The

figure of merit increased from 0.55 at a density of 0.0120 kg/m^3 to 0.59 at a density of 0.0185 kg/m^3.

a)

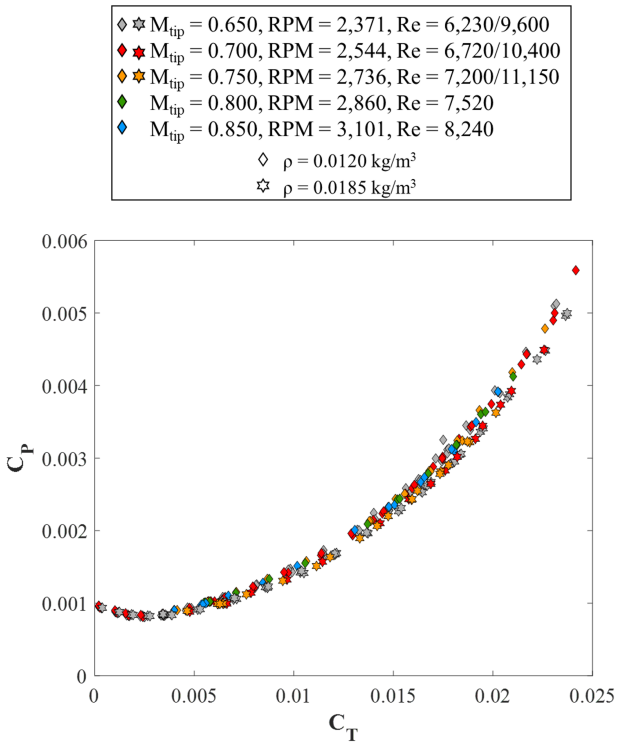

b)

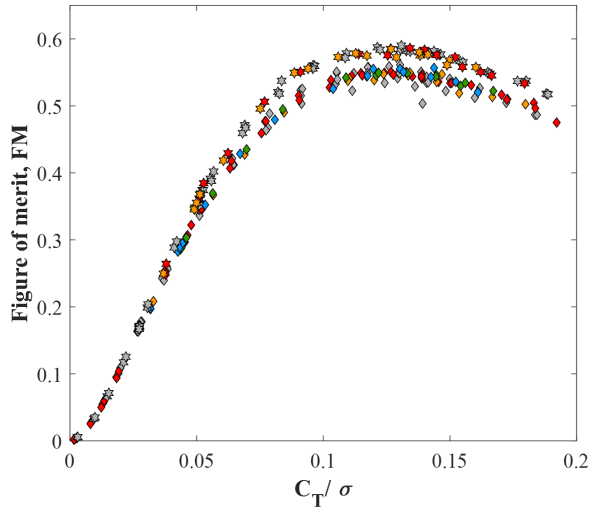

Figure 13. a) Coefficient of power versus coefficient of thrust and b) figure of merit versus blade loading for SRH coaxial rotor configuration.

Figure 14 shows collective as a function so blade loading for the SRH rotor. As collective increases, blade loading also increases. In general, a higher blade loading was seen at a density of 0.0185 kg/m^3 compared to a density of 0.0120 kg/m^3 for all rotational speeds. For example, at a density of 0.0120 kg/m^3, 8 degrees collective, and 2,371 RPM, a blade loading of 0.0788 is seen; whereas the same RPM and collective condition at at a density of 0.0185 kg/m^3 yields a higher blade loading of 0.0821.

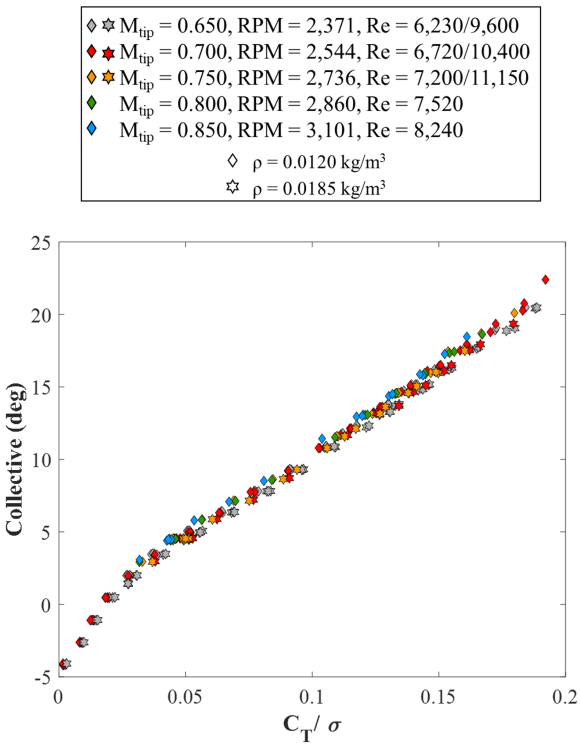

Figure 14. Blade loading versus collective pitch for SRH coaxial rotor configuration.

Figure 15 compares figure of merit for EDM-1 without the cruciform box and the DRT performance results, highlighting the improved performance for an increased rotor diameter. RPM was not matched between the two tests and therefore a slight difference in RPM is shown for a density of 0.0185 kg/m^3. Performance results from the DRT campaign satisfied MSR rotor performance requirements, and thus no additional blade design iterations are needed moving forward.

Data Quality

An uncertainty propagation analysis was performed on all DRT data in order to address concerns regarding the large fluctuations illustrated in the grayed data windows (Figure 11). For each point in the SRH dual rotor data set, an uncertainty propagation analysis was performed to determine the uncertainties in the calculated figure of merit and blade loading.

Performing an uncertainty propagation analysis defines the amount of uncertainty or error expected in the averaged data set (Ref. 6). Equation 1 is the standard form of the uncertainty propagation equation (Ref. 6). Parameters in the standard form include: calculated value derived from measurements (y), value for measurement $i(x_i)$, number of measurement

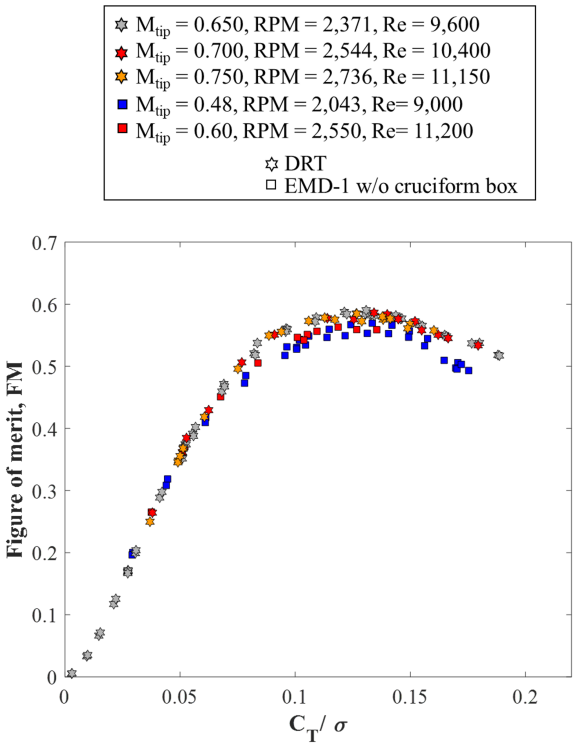

Figure 15. Figure of merit versus blade loading for EDM-1 without the cruciform box and SRH coaxial rotor configuration.

variables (N), standard deviation of the uncertainty for measurement $x_i(u(x_i))$, standard deviation of the correlated uncertainty for measurements $(u'(x_i,x_j))$, x_i and x_j $(u'(x_i,x_j))$, and variance of the combined uncertainties for y $(u_c^2(y))$.

$$u_c^2(y) = \sum_{i=1}^{n} \left(\frac{\partial y}{\partial x_i}\right)^2 u^2(x_i) + 2\sum_{i=1}^{N-1}\sum_{j=i+1}^{N} \frac{\partial y}{\partial x_i}\frac{\partial y}{\partial x_j} u\prime(x_i,x_j) \quad (1)$$

For data that is unfiltered, the standard error of the mean, $\sigma_{\bar{x}}$, is calculated solely by the number of points in the sample. If the data is filtered, the data points are no longer statistically independent, so the filter setting must be considered (Equation 2), where f_b is the filter frequency setting and t is the time length of the sample (Ref. 7).

$$\sigma_{\bar{x}} = \frac{\sigma_x}{\sqrt{N}} = \frac{\sigma_x}{\sqrt{2 f_b t}} \quad (2)$$

Variables that are averaged during post processing require an uncertainty propagation analysis. Figure of merit is calculated using coefficient of power and thrust, see Equations 3 through 5. For figure of merit, the thrust, power, and rotational speed were acquired and averaged over a time window. Rotational speed is only included for uncertainty propagation results for blade loading and not figure of merit.

$$FM = \frac{{C_T}^{3/2}}{\sqrt{2}C_P} \quad (3)$$

$$C_T = \frac{T}{\rho A\,(\Omega R)^2} \quad (4)$$

$$C_P = \frac{P}{\rho A(\Omega \mathrm{R})^3} \quad (5)$$

Uncertainty propagation analysis highlighted many areas across test conditions and configurations where unsteadiness in test data may have influenced the results. As a result, the final propagation uncertainty equations for figure of merit and blade loading are shown in Equations 6 and 7, respectively.

$$FM = FM \pm 2\sqrt{\left(\frac{\partial FM}{\partial T}\,\bar{\sigma}_T\right)^2 + \left(\frac{\partial FM}{\partial P}\,\bar{\sigma}_P\right)^2} \quad (6)$$

$$\frac{C_T}{\sigma} = \frac{C_T}{\sigma} \pm 2\sqrt{\left(\frac{\partial \frac{C_T}{\sigma}}{\partial T}\,\bar{\sigma}_T\right)^2 + \left(\frac{\partial \frac{C_T}{\sigma}}{\partial \Omega}\,\bar{\sigma}_\Omega\right)^2} \quad (7)$$

For the coaxial rotor configuration (Fig. 16), greater uncertainty for a loading greater than 0.11 is shown for all tip speeds due to unsteadiness in torque and thrust for a density of 0.0185 kg/m^3. A slightly larger uncertainty is shown at a density of 0.0120 kg/m^3, see Fig. 17. The unsteadiness observed in the torque and thrust might possibly be due to summing two load cells together for thrust and torque, or from the inflow of one or both rotors.

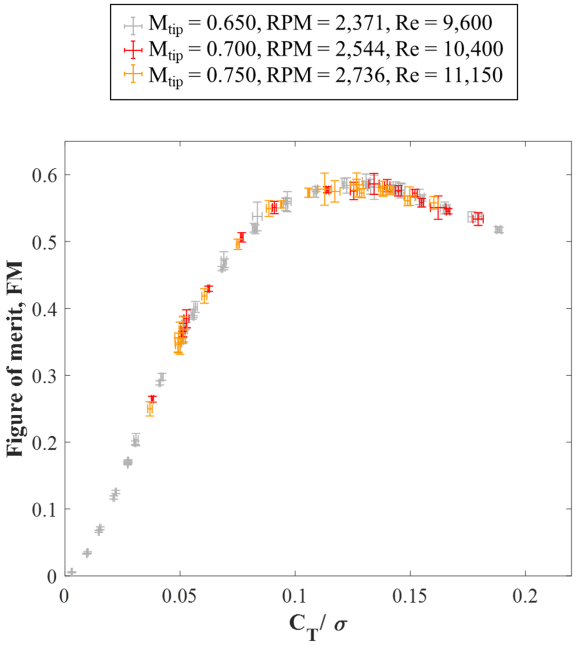

Figure 16. Figure of merit versus blade loading for DRT coaxial rotor configuration with uncertainty at ρ = 0.0185 kg/m^3.

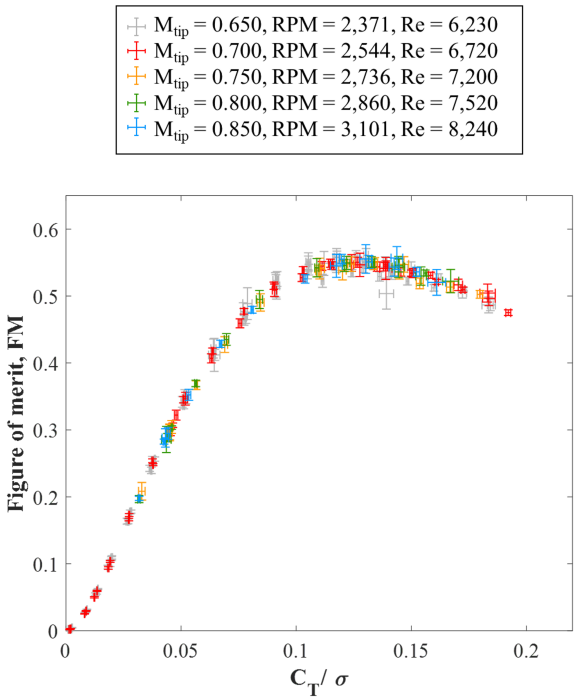

Figure 17. Figure of merit versus blade loading for DRT coaxial rotor configuration with uncertainty at ρ = 0.0120 kg/m^3.

CONCLUSIONS

Engineering Design Model 1 (EDM-1), Transonic Rotor Test (TRT), and Dual Rotor Test (DRT) campaigns were conducted at the NASA Jet Propulsion Laboratory in the 25-ft Space Simulator in support of the NASA and ESA Mars Sample Return mission. EDM-1 and TRT used Ingenuity rotors, and test results showed even with increased collective and RPM, the heritage rotors would not be sufficient to meet SRH mission requirements. As a result, the larger radius and optimized planform SRH rotor was created and tested in DRT. Experimental performance data was collected on the two different sets of blades at various rotational speeds and densities in coaxial and single rotor configurations.

For the coaxial rotor configuration in the Dual Rotor Test (DRT) campaign, increasing RPM revealed no significant drag divergence or stall at high tip Mach numbers. It was concluded that tip speeds could be safely increased beyond heritage Ingenuity limits into the transonic range for additional lift capability, thereby expanding the operational mission envelope.

Comparing results from EDM-1 without the cruciform box to the SRH coaxial configuration, it was concluded that an increase in performance was achieved using the optimized SRH rotor design. Results from all three campaigns will aid in future Mars rotorcraft development by providing data for validation efforts.

AUTHOR CONTACT

Natasha Schatzman
Natasha.Schatzman@nasa.gov

Athena Chan
Athena.Chan@nasa.gov

Michael Fillman
Fillman@avinc.com

Larry Meyn
Larry.Meyn@nasa.gov

Vinod Gehlot
Vinod.P.Gehlot@jpl.nasa.gov

Kenneth Glazebrook
Kenneth.J.Glazebrook@jpl.nasa.gov

Diego Santillan
Diego.Santillan.Castillo@jpl.nasa.gov

Paulina Ridland
Paulina.Ridland@avinc.com

ACKNOWLEDGMENTS

Authors would like to acknowledge the entire Mars Sample Return program team for all their support. Special thanks to Wayne Johnson for his mentorship and our reviewers Stephen Wright and Lauren Weist. The authors acknowledge the Mars Sample Return Project, NASA's Jet Propulsion Laboratory, NASA Ames Research Center, NASA Langley Research Center, AeroVironment, and the NASA Convergent Aeronautics Solutions (CAS) Project for funding and support. Experimental efforts were performed at the Jet Propulsion Laboratory, California Institute of Technology, under a contract with the National Aeronautics and Space Administration.

The decision to implement Mars Sample Return will not be finalized until NASA's completion of the National Environmental Policy Act (NEPA) process. This document is being made available for information purposes only.

REFERENCES

1. Schatzman, N., Chan, A., Gehlot, V., and Glazebrook, K., "Data Processing and Analysis of Performance Measurements from Ingenuity Rotors in the Jet Propulsion Laboratory 25-ft Space Simulator", Vertical Flight Society's Transformative Vertical Flight (TVF) 2024 meeting, Santa Clara, CA, February 6–8, 2024.

2. Sarli, B., Gough, K., Hagedorn, A., Bowman, E., Rondey, J., Yew, C., Neuman, M., Green, T., Lin, J., Cataldo, G. and Hudgins, P., "NASA Capture, Containment, and Return System: Bringing Mars Samples to Earth." 34th International Symposium on Space Technology and Science. 2023.

3. Harrell, J. W., and Argoud, M. J., "The 25-ft Space Simulator at the Jet Propulsion Laboratory," NASA CR 106222, October 1969.

4. MATLAB, version 9.14.0.2206163 (R2023a), The MathWorks Inc., Natick, Massachusetts, 2010.

5. Johnson, W., *Rotorcraft Aeromechanics*, New York: Cambridge University Press, 2013.

6. Taylor, B. N. and Kuyatt, C. E., Guidelines for Evaluating and Expressing the Uncertainty of NIST Measurement Results, National Institute of Standards and Technology, NIST technical note 1297, September 1994.

7. Bendat, J. S. and Piersol, A. G., *Random Data: Analysis and Measurement Procedures*, John Wiley and Sons, Inc., 1971.